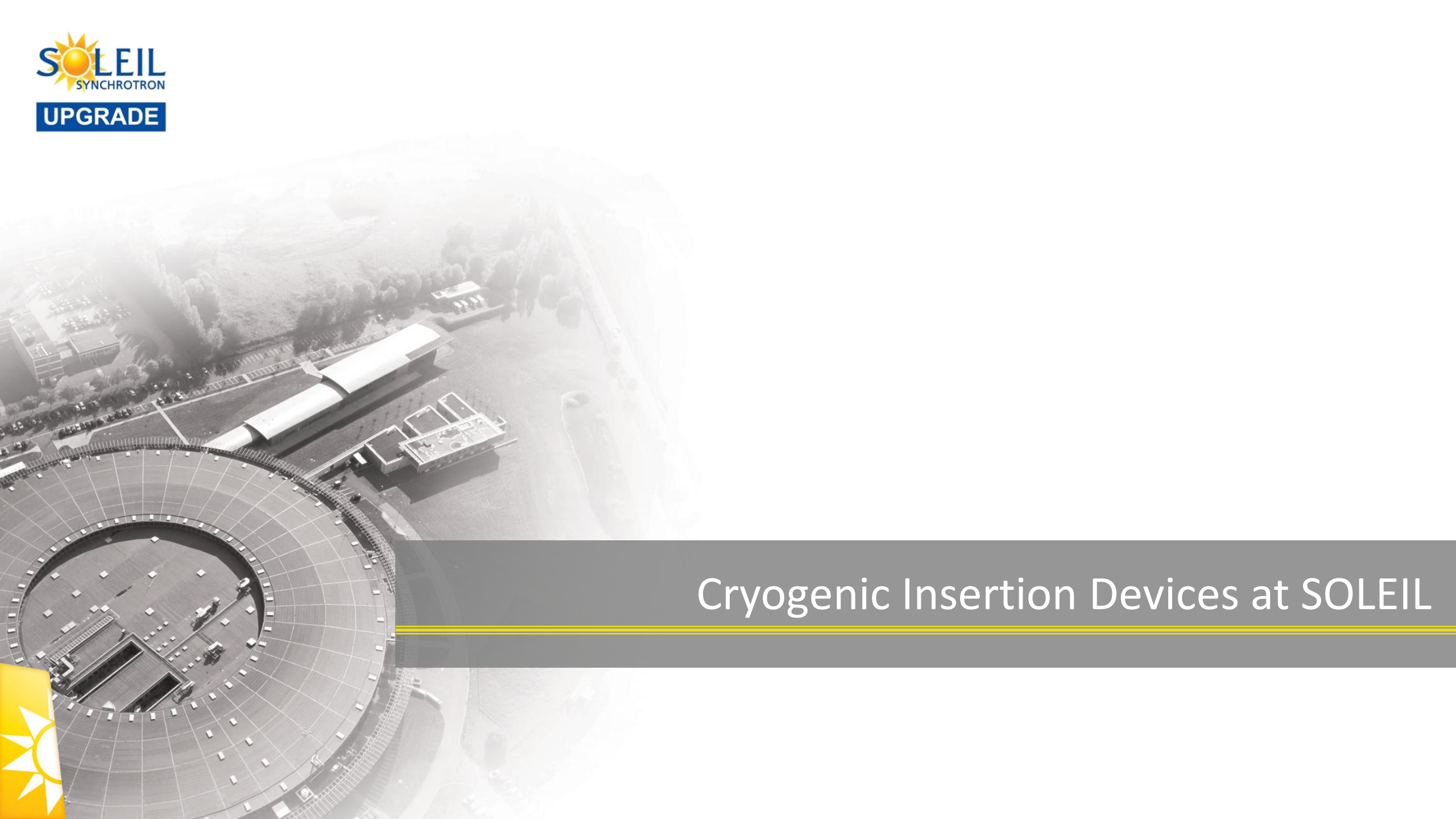

Cryogenic Insertion Devices at SOLEIL

Generalities

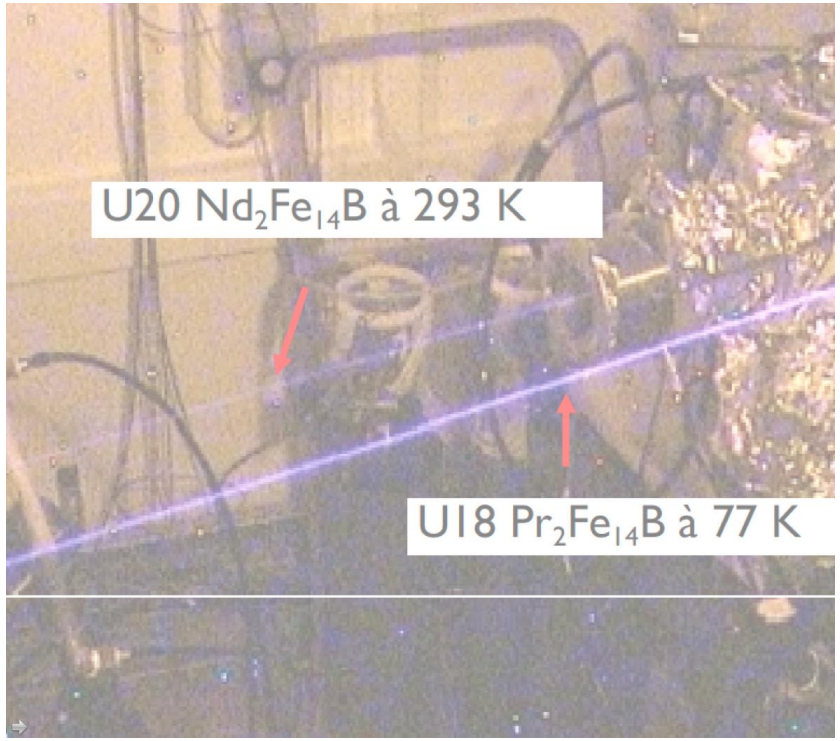

Figure 1 : *Photon beams from a standard in-vacuum ID and a cryogenic ID*

Generalities

SOLEIL I parameters

- 3rd generation light source
- Energy : 2.75 GeV
- Current : 500 mA
- Emittance: 3.9 nm.rad
- Energy spread : 0.1%
- Coupling : 1%

SOLEIL II parameters

- 4th generation light source
- Energy : 2.75 GeV
- Current : 500 mA
- Emittance: 80 pm.rad
- Energy spread : 0.1%
- Coupling : 1%

Figure 2 : *Synchrotron SOLEIL buildings*

Figure 3 : *HU640*

Figure 4 : *HU256*

Beamline	Source	Period (mm)	Nb. periods	Gap (mm)	Bz (T)	Bx (T)
Désirs	HU640	640	14	19	0.11	0.09
Cassiopée	HU256	256	12	50 (H) 15 (V)	0.40	0.28
Pléiades	HU256	256	12	50 (H) 15 (V)	0.40	0.28
Antarès	HU256	256	12	50 (H) 15 (V)	0.40	0.28
Deimos	HU65	65	24	15.5	0.25	0.25 (PM)

Table 1 : *List of electromagnetic devices installed on SOLEIL I storage ring*

Generalities

Beamline	Source	Type	Period (mm)	Nb.	Gap (mm)	Bz (T)	Bx (T)	PM Grade
Tempo	HU80	Apple II	80	19	15.5	0.98	0.75	NdFeB
Pléiades	HU80	Apple II	80	19	15.5	0.98	0.75	NdFeB
Sextants	HU80	Apple II	80	19	15.5	0.98	0.75	NdFeB
Hermès	HU64	Apple II	64	25	15.5	0.86	0.62	NdFeB
Cassiopée	HU60	Apple II	60	27	15.5	0.8	0.55	NdFeB
Antarès	HU60	Apple II	60	27	15.5	0.8	0.55	NdFeB
Deimos	HU52	Apple II	52	31	15.5	0.77	0.52	NdFeB
Lucia	HU52	Apple II	52	31	15.5	0.77	0.52	NdFeB
Tempo	HU44	Apple II	44	36	15.5	0.64	0.4	NdFeB
Sextants	HU44	Apple II	44	36	15.5	0.64	0.4	NdFeB
Sextants	HU42	Apple II	42	34	15.5	0.58	0.37	NdFeB
Sirius	HU36	Apple II	36	44	15.5	0.75	0.53	NdFeB

Table 2 : *List of PM devices providing helical polarization installed on SOLEIL I storage ring*

Figure 5 : *APPLE II ID*

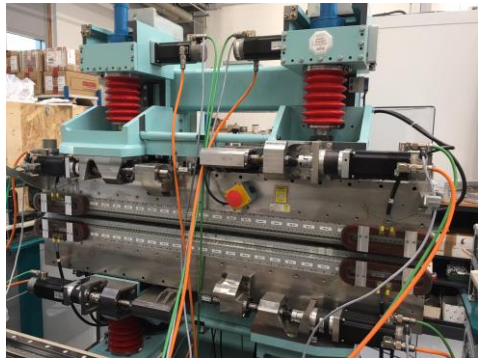

Figure 6 : *8-axis APPL EII ID*

Generalities

Beamline	Source	Type	Period (mm)	Nb.	Gap (mm)	Bz (T)	Bx (T)	PM Grade
PX2	U24	In-vacuum	24	80	5.5	0.84		NdFeB
PX1	U20	In-vacuum	20	106	5.5	0.96		SmCo
Cristal	U20	In-vacuum	20	106	5.5	0.96		SmCo
Swing	U20	In-vacuum	20	106	5.5	0.96		SmCo
Sixs	U20	In-vacuum	20	106	5.5	0.96		SmCo
Spare (x1)	U20	In-vacuum	20	106	5.5	0.96		SmCo
Spare (x2)	U20	In-vacuum	20	106	5.5	1.06		NdFeB
Galaxies	U20	In-vacuum	20	106	5.5	1.06		NdFeB
Psyché	WSV50	In-vacuum wiggler	50	40	5.5	2.1		NdFeB
Puma	W164	Out-vacuum Wiggler	164	20	15.5	1.8		NdFeB
Nanoscopium	U18	Cryogenic	18	106	5.5	1.16		PrFeB
Anatomix	U18	Cryogenic	18	106	5.5	1.16		PrFeB
Coxinel	U18	Cryogenic	18	106	5.5	1.16		PrFeB
R&D	U15	Cryogenic	15	200	3	1.16		PrFeB

Table 3 : *List of PM devices providing linear horizontal polarization installed on SOLEIL I storage ring*

Figure 7 : *In-vacuum Wiggler*

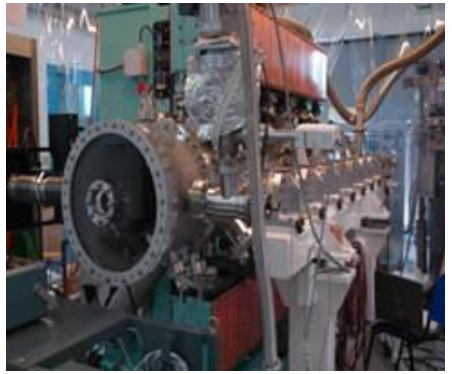

Figure 8 : *Cryogenic undulator*

Generalities

High energy photons produced by the in-vacuum undulators IVUs

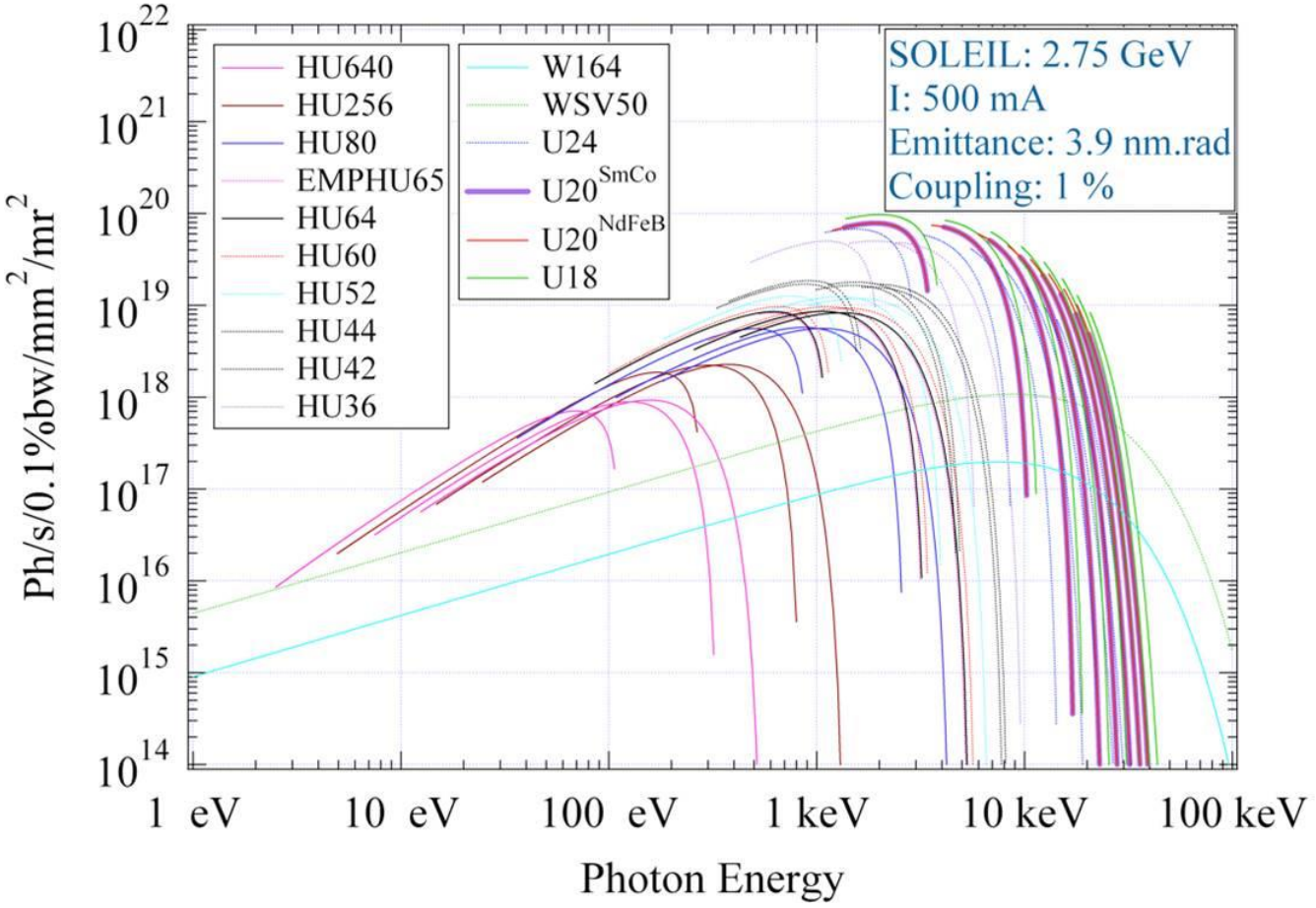

Figure 9 : *Brightness produced by SOLEIL I IDs*

How to gain brightness at high energies?

Generalities

Reaching more brightness at high energies implies

➔ more interferences : increasing the total nb of periods

- ❑ building longer IDs
- ❑ Reducing the period length

➔ higher peak field : **cryogenic undulators**

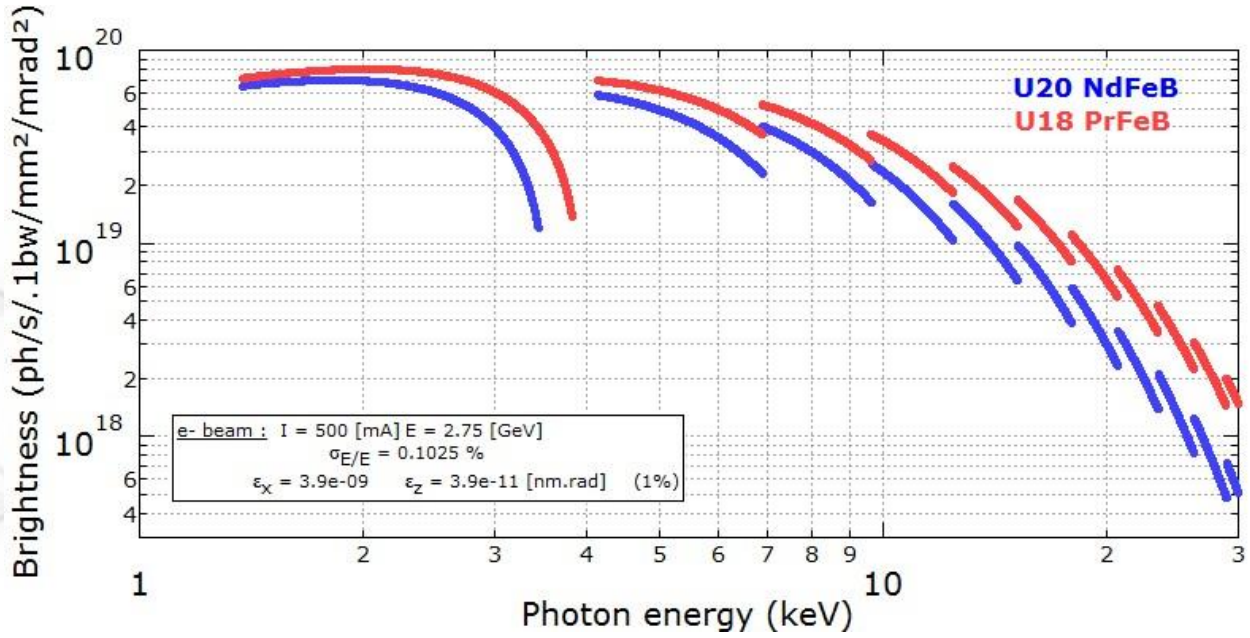

Figure 10 : *Brightness of a 20 mm period NdFeB undulator compared with a 18 mm period PrFeB cryogenic undulator*

Factor of 3 at 30 keV on the brightness

Cryogenic undulators at SOLEIL

- CPMU18 n°1 : installed for Nanoscopium long beamline in 2011
- CPMU18 n°2 : used for COXINEL since 2015 and will be installed on Cristal beamline in 2024
- CPMU18 n°3 : installed for Anatomix long beamline in 2017
- CPMU15 : under construction

Figure 11 : *CPMU18 undulators in the SOLEIL I ring, dedicated to Anatomix & Nanoscopium beamlines*

Magnetic design

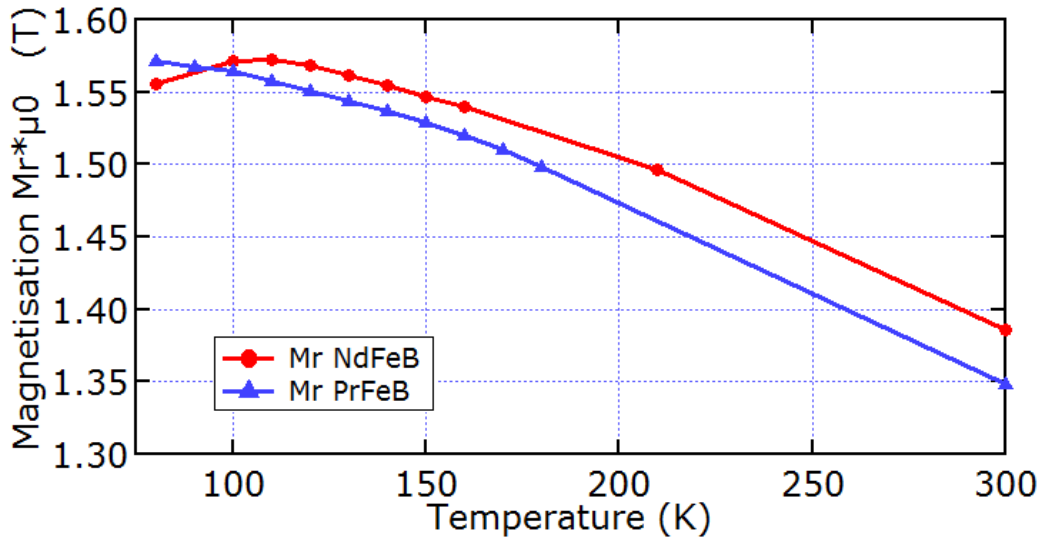

Figure 12 : *Dependance of magnets remanent field with temperature*

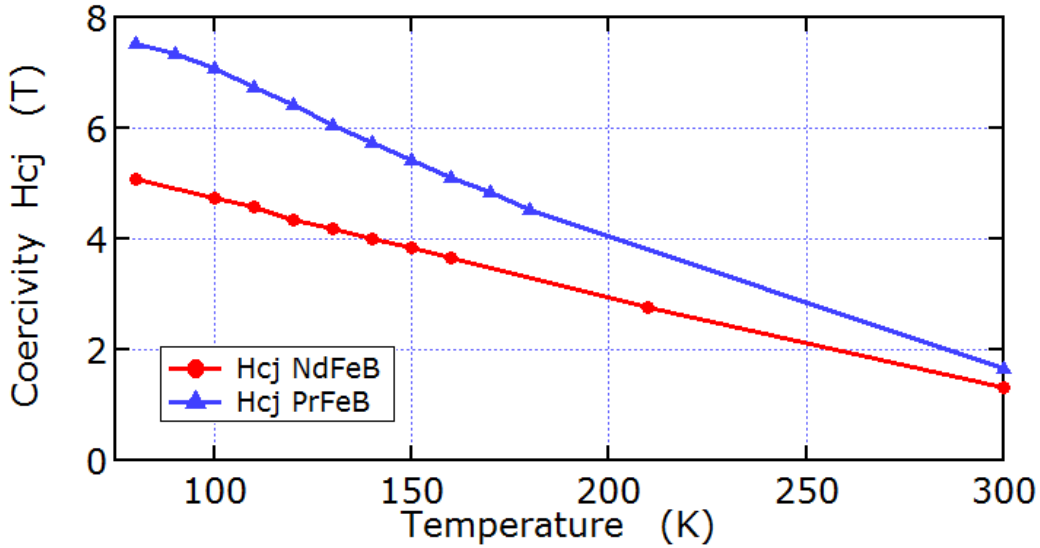

Figure 13 : *Dependance of magnets coercivity with temperature*

NdFeB magnets

- Undergoes SRT below 120 K
- Coercivity keeps increasing
- Heaters have to be installed along the ID
- B_r variation at 77 K : -0.1%/K

PrFeB magnets

- Can be cooled down directly to 77 K
- Reaches higher field
- Coercivity keeps increasing
- B_r variation at 77 K : -0.02%/K

Design

CPMU18 mechanical design

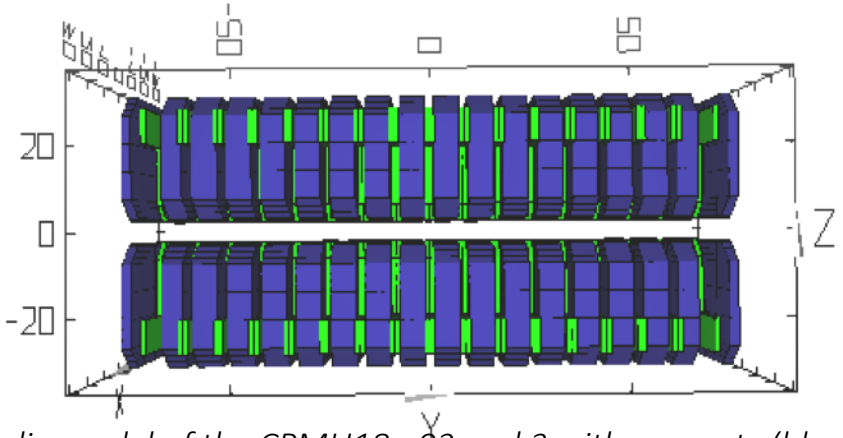

Figure 14 : *Radia model of the CPMU18 n02 and 3 with magnets (blue) and half poles (green)*

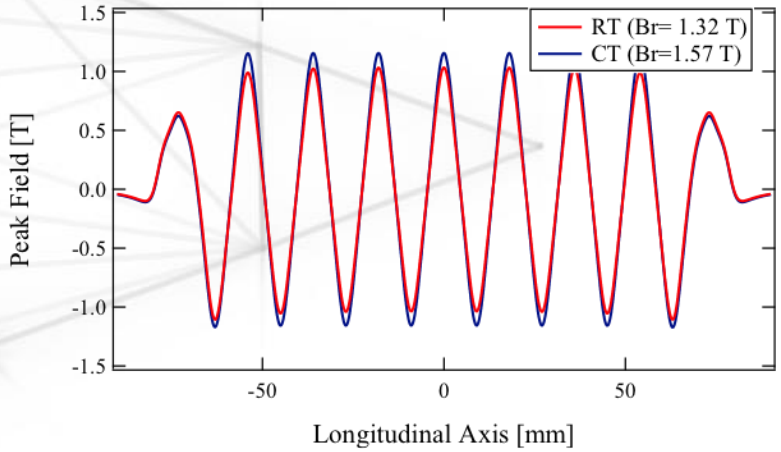

Figure 15 : *Magnetic field of the CPMU18 generated at 300 K and 77 K*

Item	Unit	Value
Technology		Hybrid
Magnet material		CR53
Remanence	T	1.35 @ 300 K
		1.57 @ 77 K
Coercivity	T	1.63 @ 300 K
		7.6 @ 77 K
Magnet size (x, z, s)	mm^3	50 × 30 × 6.5
Pole material		Vanadium Permendur
Pole size (x, z, s)	mm^3	33 × 22 × 2.5
		33 × 22 × 1.25
Period	mm	18 @ 77 K
Gap range	mm	5.5 to 30
Length	m	2
Peak field	T	1.155

Table 4 : *Main characteristics of the CPMU18*

- At 300 K, B_z = 1.005 T @ 5.5 mm
- At 77 K, B_z = 1.155 T @ 5.5 mm

CPMU18 mechanical design

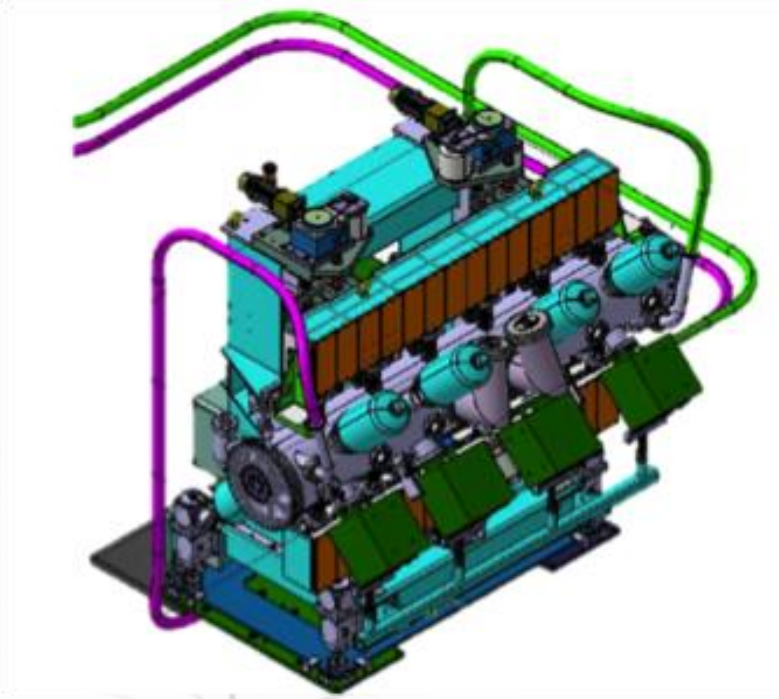

Figure 16 : *Drawing of the CPMU18 undulator*

Figure 17 : *In-vacuum girders of CPMU18*

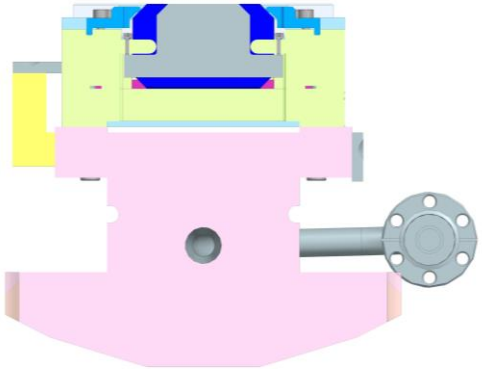

- Out/in-vacuum girders connected by 24 rods
- Cooling down by injecting LN2 through a 10mm hole in the aluminium girders
- No baking

CPMU15 mechanical design

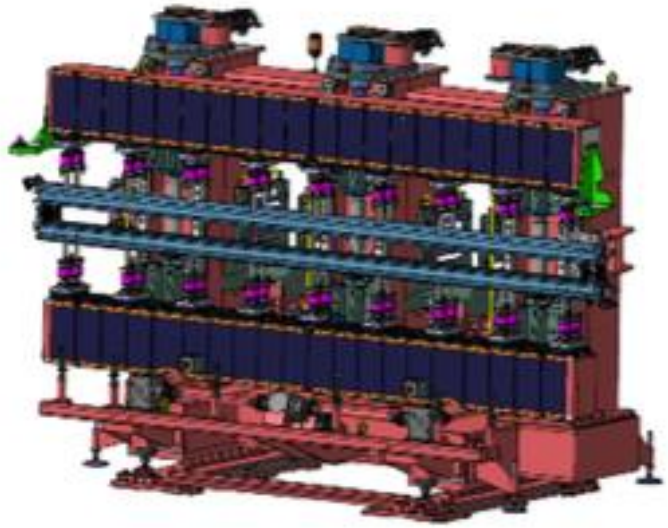

Figure 18 : *Drawing of the CPMU15 undulator*

Item	Unit	Value
Technology		Hybrid
Magnet material		CR53
Remanence	T	1.32 @ 300 K
		1.55 @ 77 K
Coercivity	kA/m	1016 @ 300 K
		1906 @ 77 K
Magnet size (x, z, s)	mm^3	50 × 30 × 5.5
Pole material		Vanadium Permendur
Pole size (x, z, s)	mm^3	33 × 22 × 1
Period	mm	15 @ 77 K
Gap range	mm	3 to 30
Length	m	3
Peak field	T	1.735

Figure 19 : *Main characteristics of the CPMU15*

- Out/in-vacuum girders connected by 36 rods
- Cooling down by injecting LN2 through a 10mm hole in the aluminium girders
- No baking

- At 300 K, B_z = 1.59 T @ 3 mm
- At 77 K, B_z = 1.735 T @ 3 mm

CPMU18 modules design

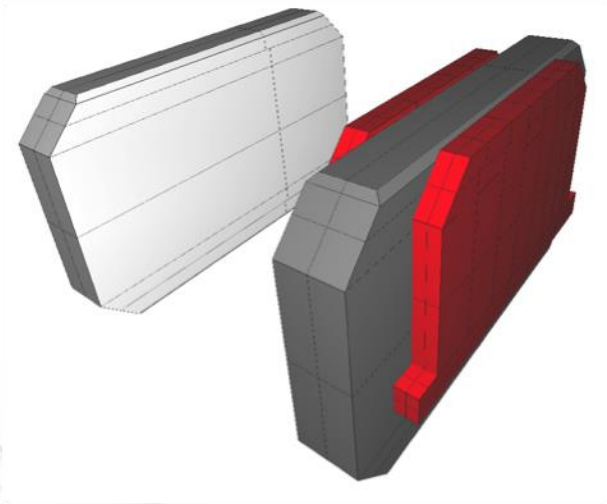

Figure 20 : *Radia model of the full pole structure of CPMU18 n°1*

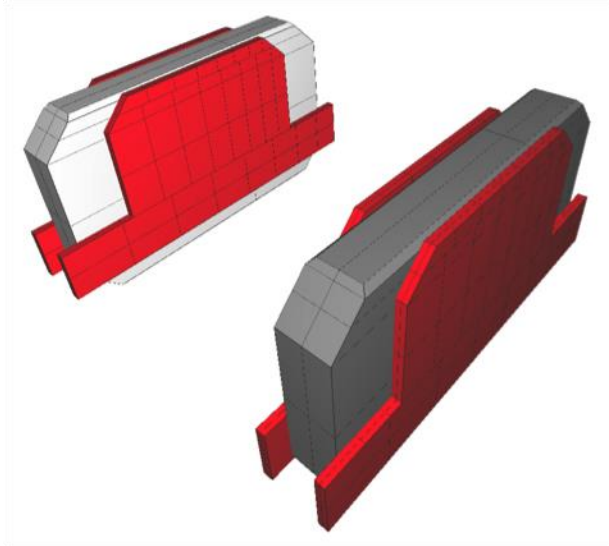

Figure 21 : *Radia model of the half-pole structure of CPMU18 n°2, 3 and CPMU15*

Advantages of the half-pole structure :

- All identical modules
- Increased number of possibilities during the assembly
- Enables swapping for magnetic corrections

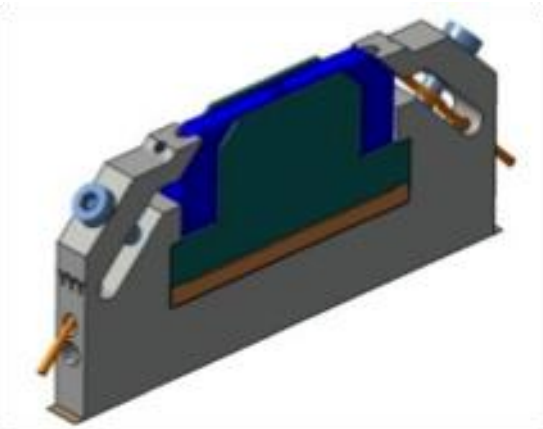

Figure 22 : *Mech. Design of holders for CPMU18 n°2, 3 and CPMU15*

Assembly at room temperature

Objective : Build an ID with an optimized phase error directly after the assembly without doing any shimming/swapping

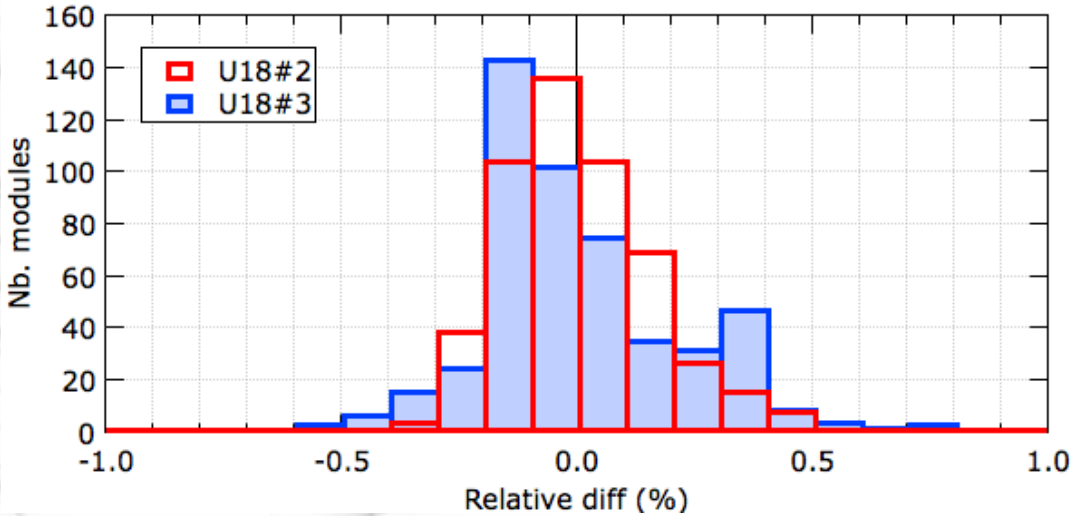

Figure 23 : *Relative difference of the total magnetic moment on magnet batch of CPMU18 n°2 & 3*

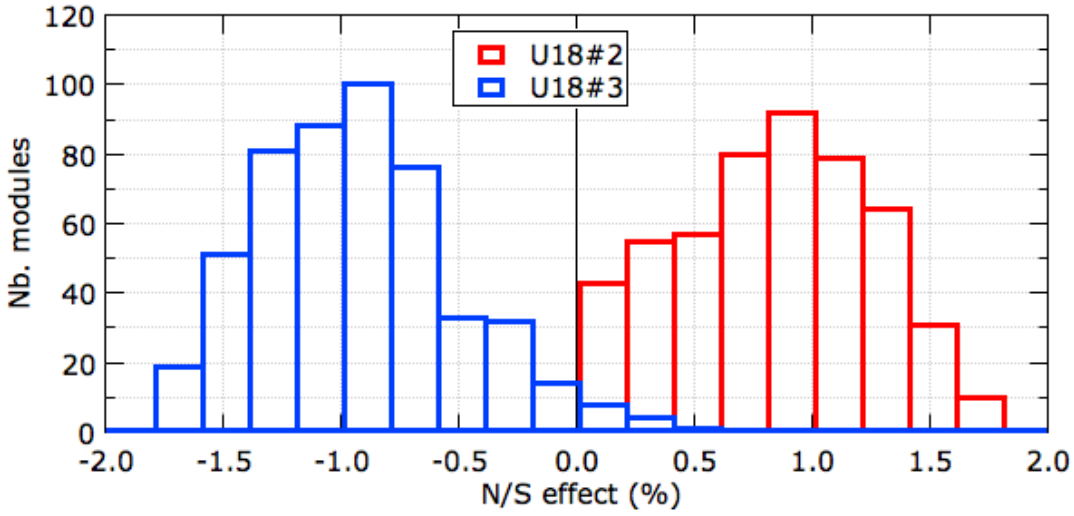

Figure 24 : *North/South effect on magnets batch of CPMU18 n°2 & 3*

Construction and optimisations

Assembly at room temperature

Figure 25 : *Hall probe and rotating coil meas.*

- Poles adjusted with 10 um copper shims
- Modules removed if
  - > 1% on average peak field
  - > 1% on N/S diff.

Figure 26 : *Robotic arm in action*

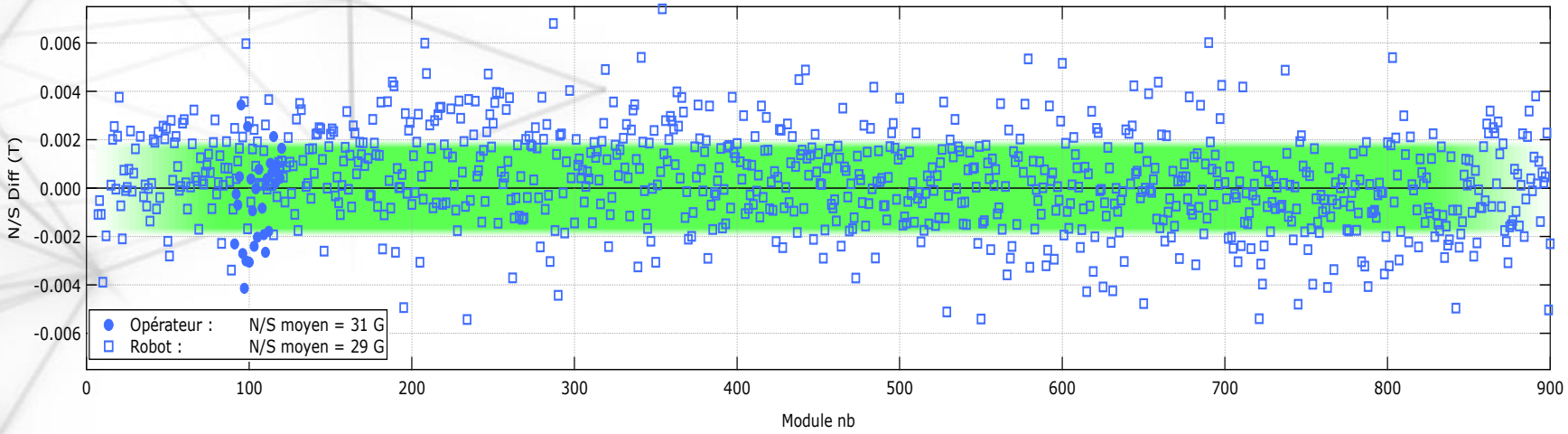

Figure 27 : *Magnetic measurements using a robotic arm*

Construction and optimisations

New magnet holder : Super-module

- Magnets are assembled first
- Then poles inserted by the bottom
- Poles can be adjusted in angle or altitude thanks to magnets using 2 screws

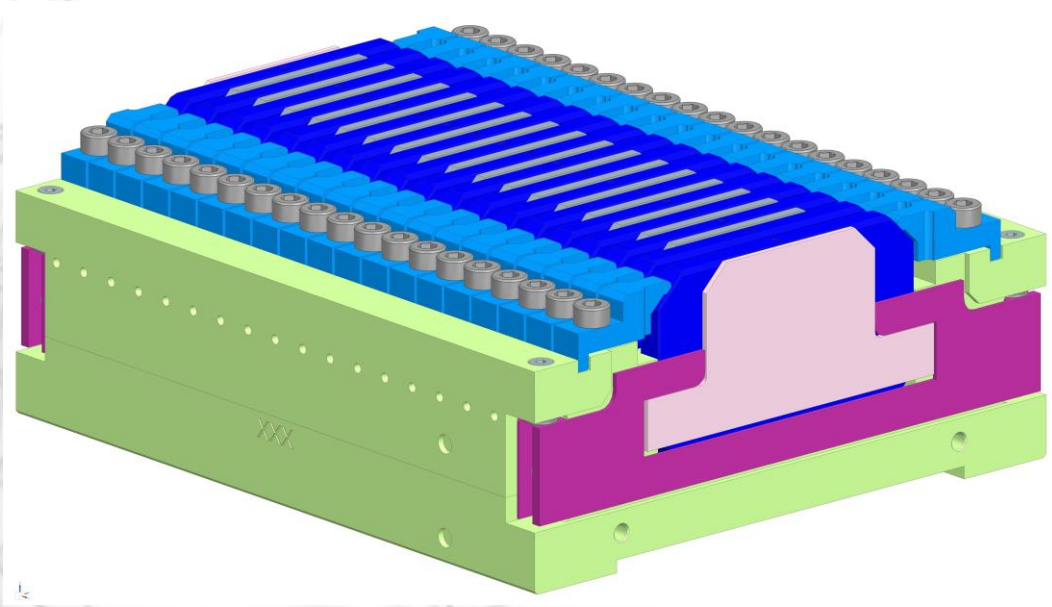

Figure 28 : *Supermodule design*

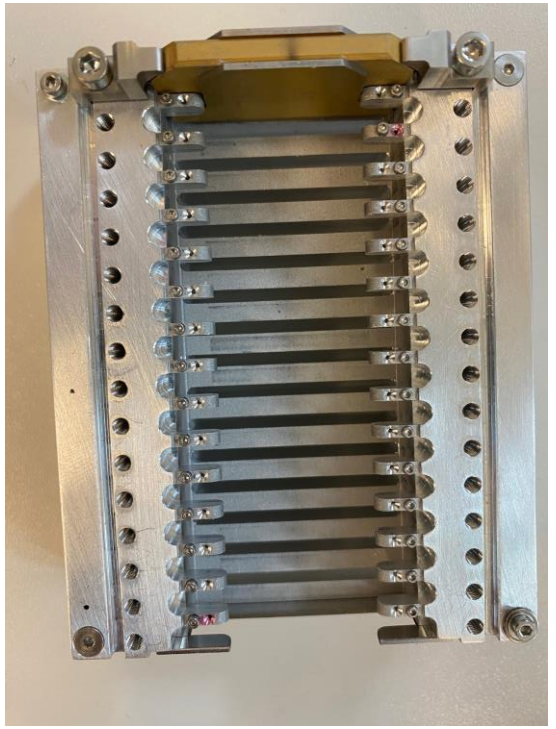

Figure 29 : *Prototypes of supermodules*

Construction and optimisations

New magnet holder : Super-module

Figure 30 : *Robotic arm adjusting a Supermodule*

This Supermodule has been designed to be fully optimized thanks to a robotic arm

- 3 lasers to measure magnets/pole
- 1 screw driver

Adjustment below 5 um with very good agreement thanks to our standard meas. tools

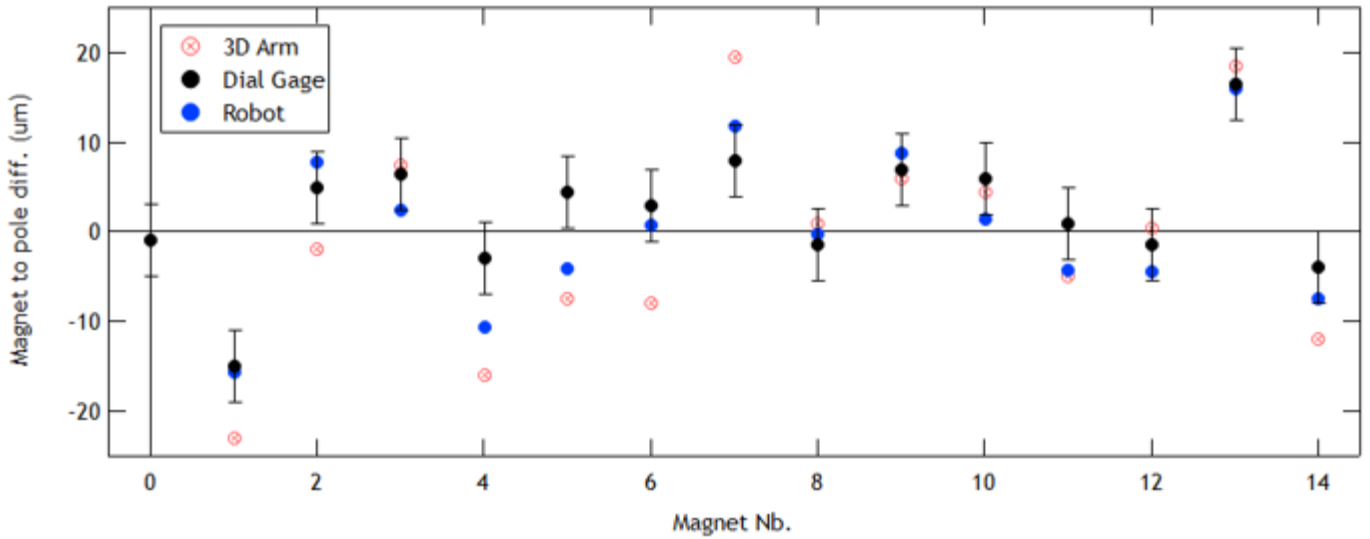

Figure 31 : *Comparison of the altitudes on a Supermodule using different tools*

Construction and optimisations

New magnet holder : Super-module

Figure 32 : *Robotic arm scanning the supermodule with a 3D Hall probe*

Magnetic adjustment using a 3D Hall probe to correct for magnetic errors

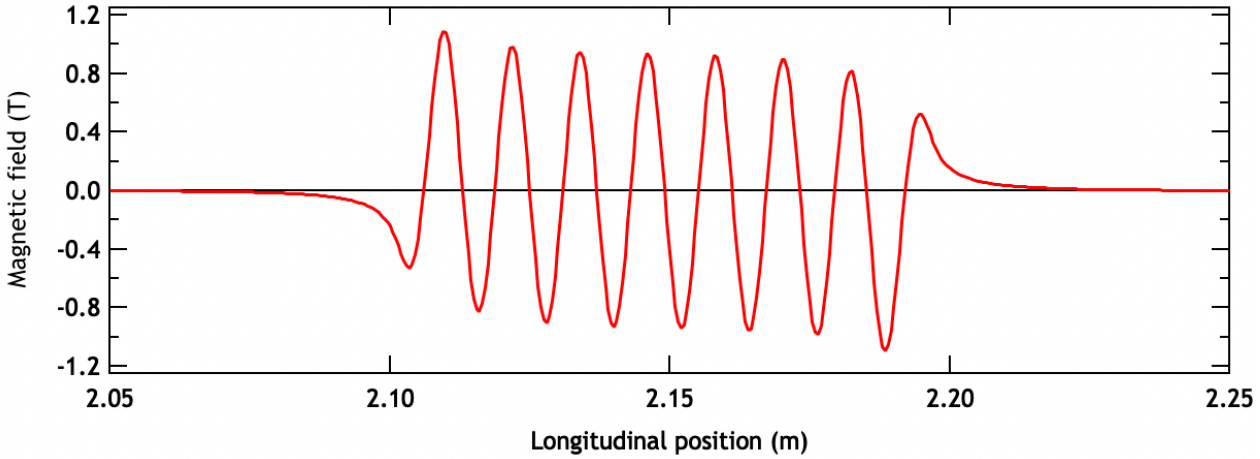

Figure 33 : *Reconstructed magnetic field profile*

Assembly of the undulator

Period by period modules are sorted and assembled on the two girders:

- 2 modules on the lower girder and 2 on the upper one
- Adjusted at +/-15 um
- Shimmed with specific values (function of the long. pos. and magnet errors)
- Measurement of all the periods
- IDBuilder >> choose the 4 convenient consecutive modules that fit defined tolerances and weight

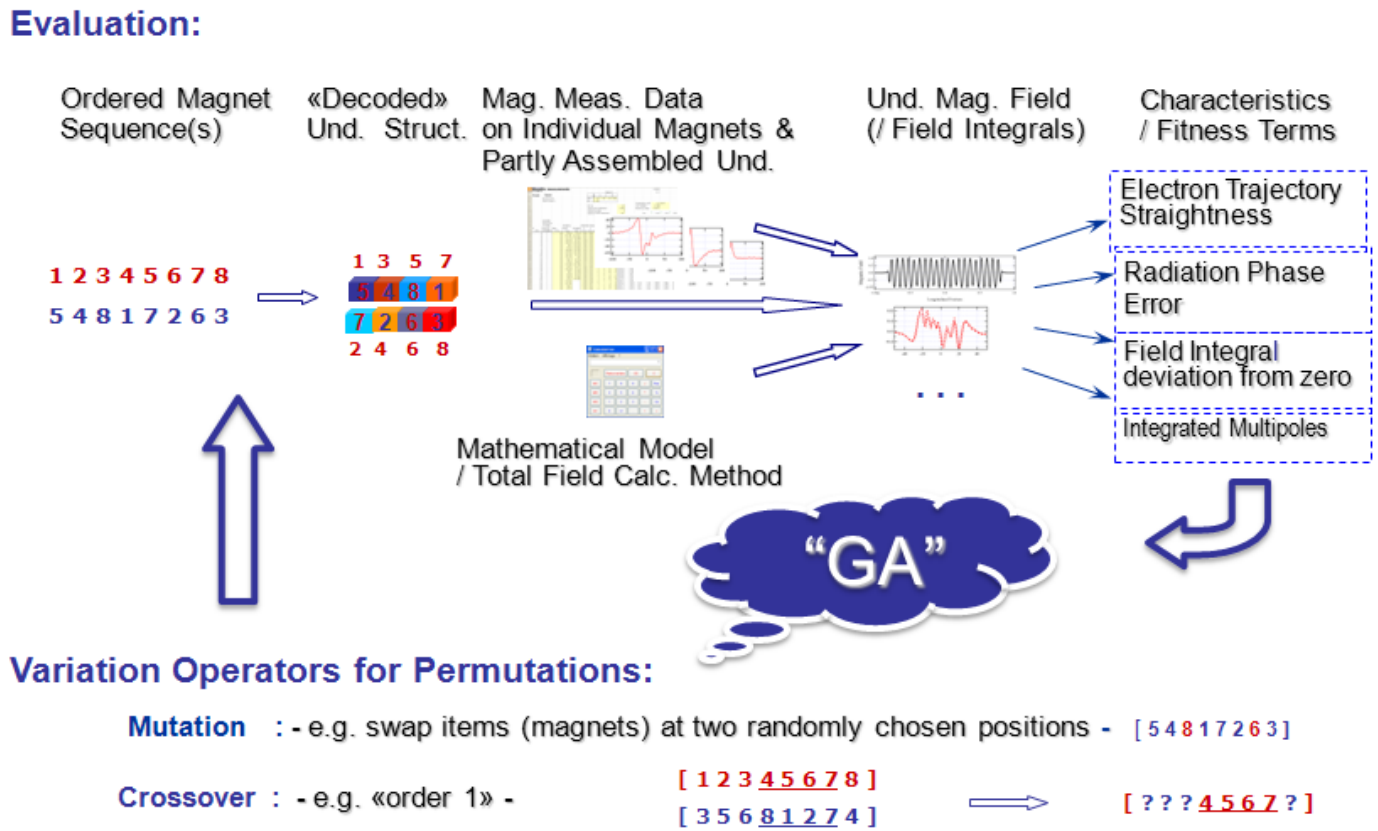

Figure 34 : *IDBuilder scheme*

Construction and optimisations

Assembly of the undulator

CPMU18 n°1
- 100 periods @ 5.5 mm
- Tapper correction
- Rods adjustments
- 92 elements shimmed

>> phase error : 2.8°

CPMU18 n°2
- 100 periods @ 5.5 mm
- Tapper correction
- Rods adjustments
- No shimming

>> phase error : 2.3°

CPMU18 n°3
- 100 periods @ 5.5 mm
- Tapper correction
- Rods adjustments
- No shimming

>> phase error : 2.45°

CPMU15 n°1
- 200 periods @ 3 mm
- Tapper correction
- Rods adjustments
- No shimming

>> phase error : 3.5°

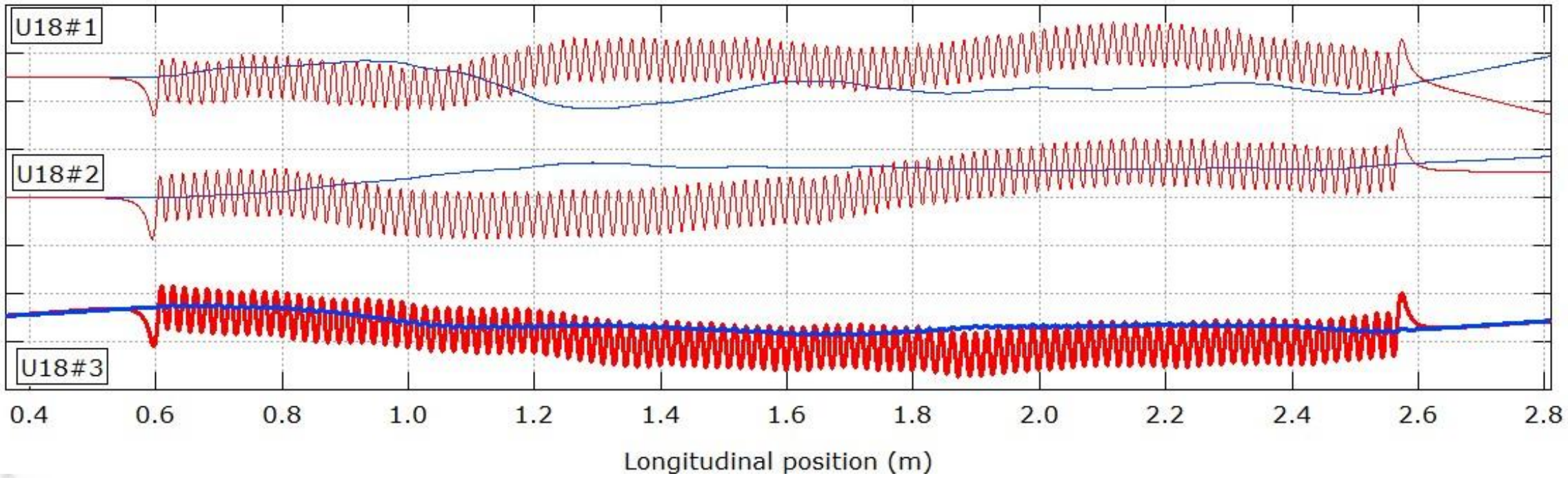

Figure 35 : *Trajectories of the CPMU18 at room temperature*

Construction and optimisations

Cooling/Warming undulators using a Cryotherm cryo-cooler

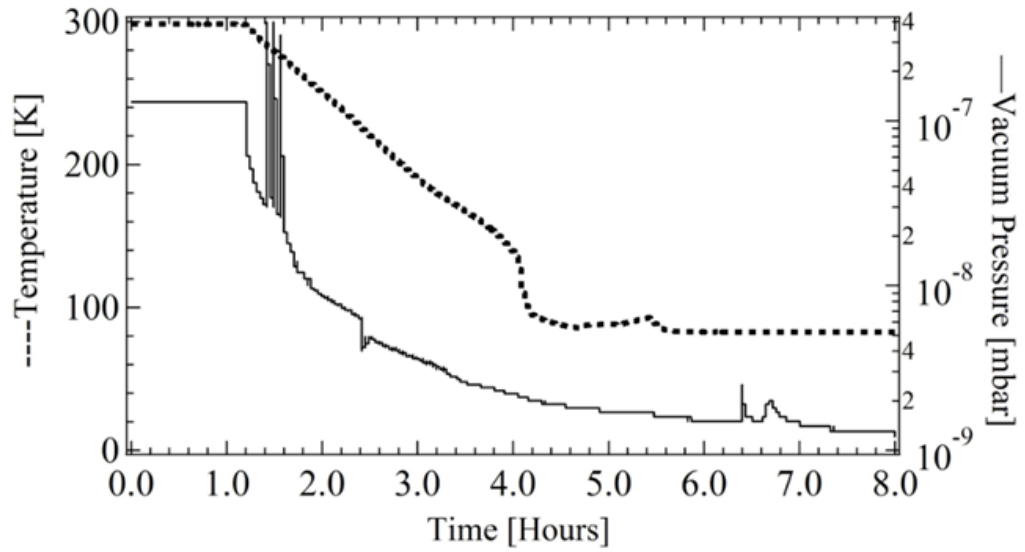

Figure 36 : *Cooling down of the undulator*

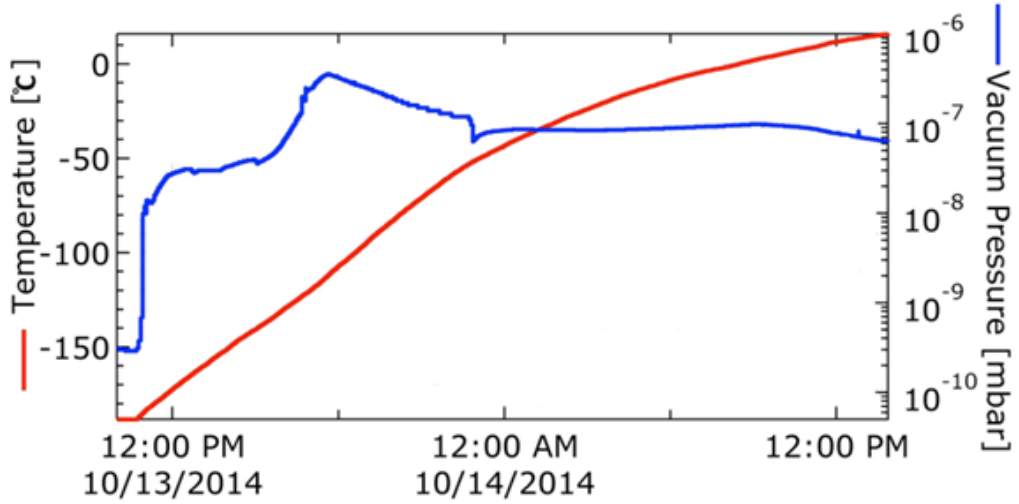

Figure 37 : *Warming up*

- 36 hours to reach 77K
- More than a decade gain on the vacuum pressure

- Natural warming : 72 hours
- Warming using nitrogen gas : 24 hours

In more than 10 years of operation only one incident impacting the beam (not due to cryo-cooler)

Construction and optimisations

Embedded measurement benches: ID correction in final configuration at 77 K

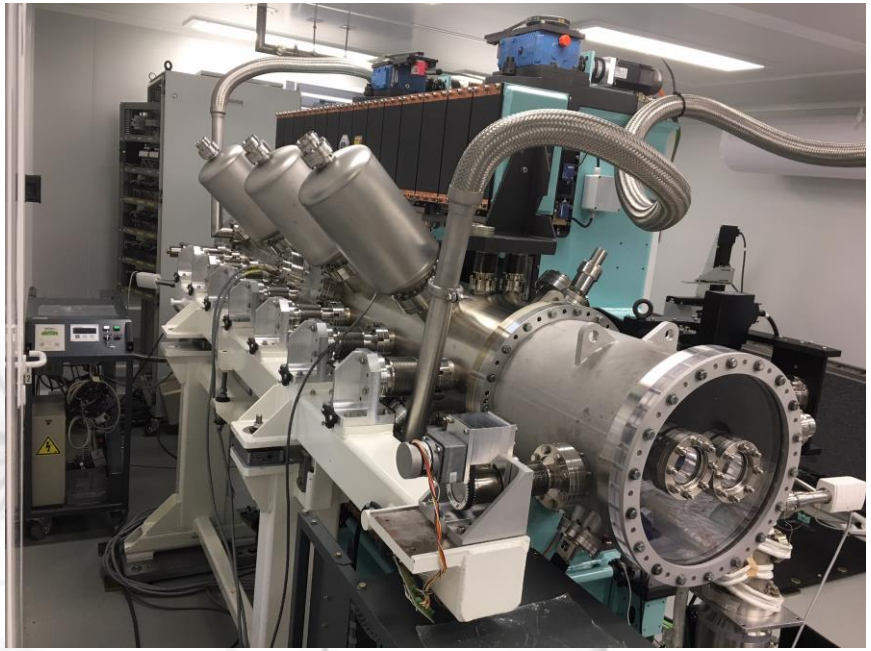

Figure 38 : *CPMU18 with in-situ Hall probe bench*

- Hall probe installed on a carriage
- Stepper motor via magn. Coupling
- Girder thermalized
- Heidenhein encoder for long.pos
- Triggers from Renishaw interferrometer

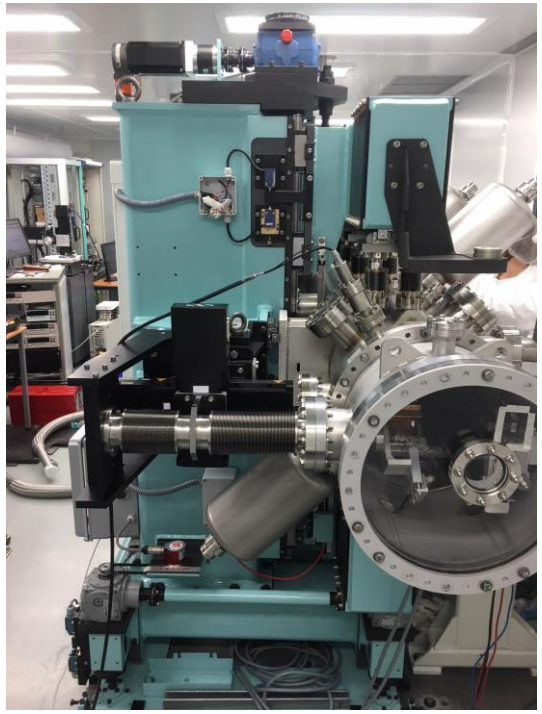

Figure 39 : *CPMU18 with in-situ stretched wire bench*

- 100 um tungsten wire
- Stretched under 10 N
- Keithley 2182A nanovoltmeter

Mechanical changes at 77 K

- Gap opening due to rods contraction : 1.3 mm (wire measurements)
  - Magn. gap @ 300 K : 5.5 mm
  - Mech. gap @ 300 K : 5 mm with stretched wire
  - Mech. gap @ 77 K : 6.3 mm with stretched wire
- Girders long. contractions (12 mm) : period reduced from 18.16 to 18.04 mm

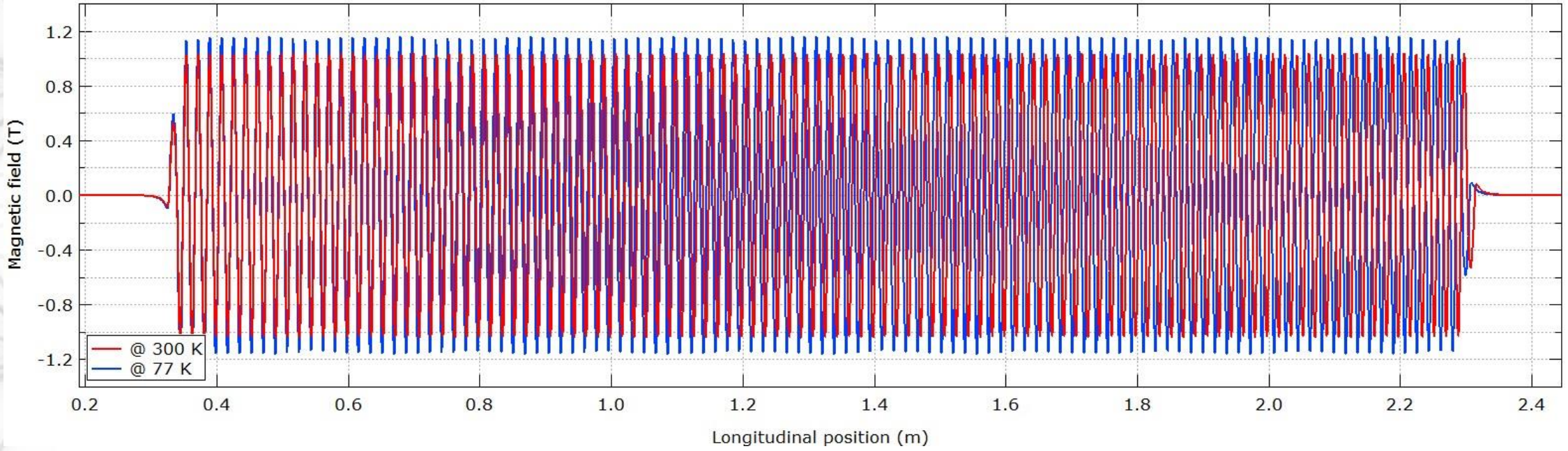

Figure 40 : *Vertical magnetic field profiles @ 330 K and 77 K after gap correction*

Construction and optimisations

Rods adjustments >>. Phase error reduction from 10 to below 3°

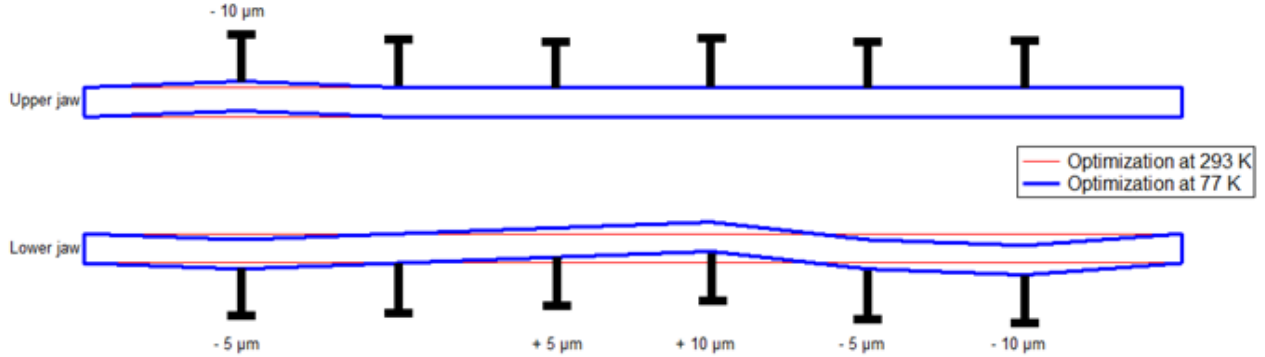

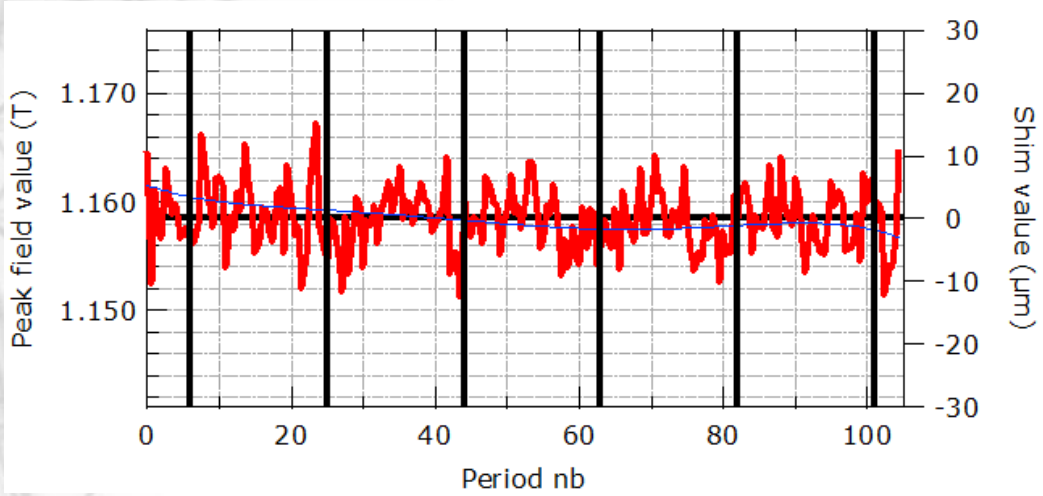

Figure 41 : *Abs. values of the peak field versus long. position before rods adjustments*

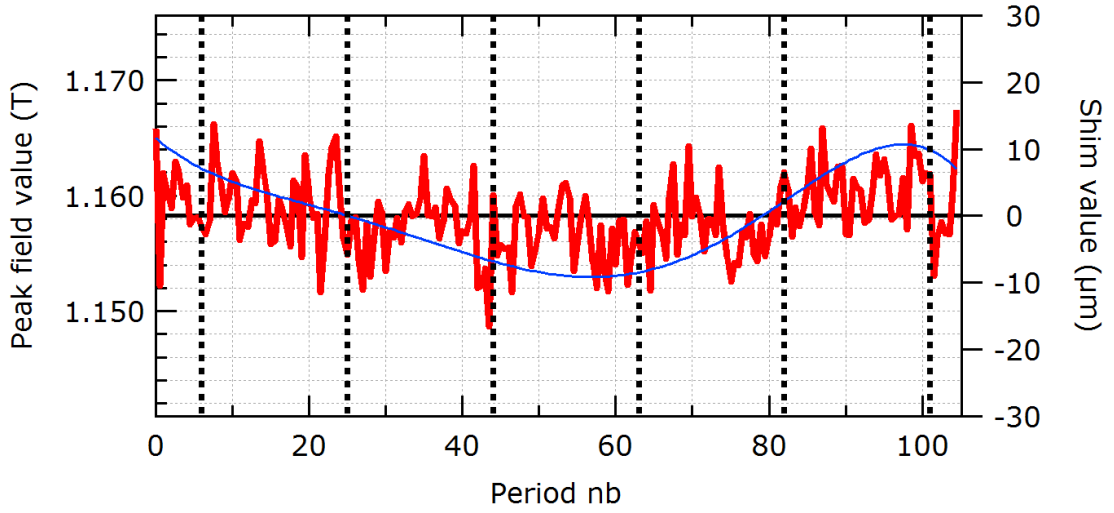

Figure 42 : *Abs. values of the peak field versus long. position after rods adjustments*

Construction and optimisations

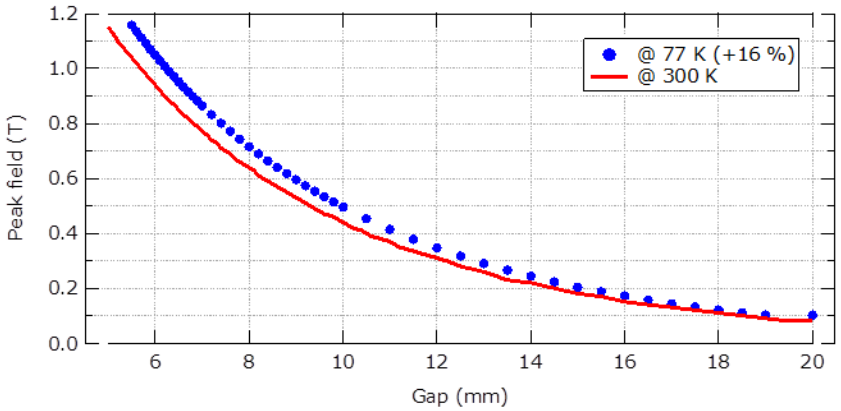

Figure 43 : *Vert. peak field vs gap at 300 K and 77 K*

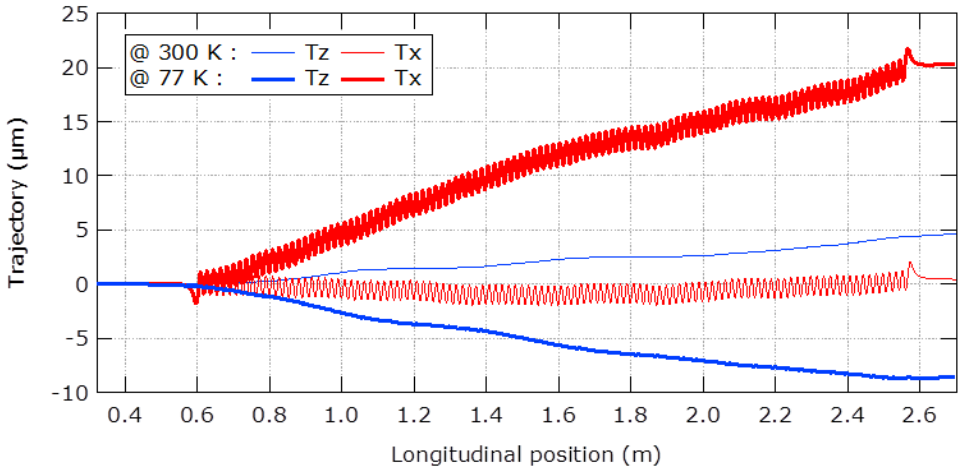

Figure 44 : *H and V trajectories at 300 K & 77 K*

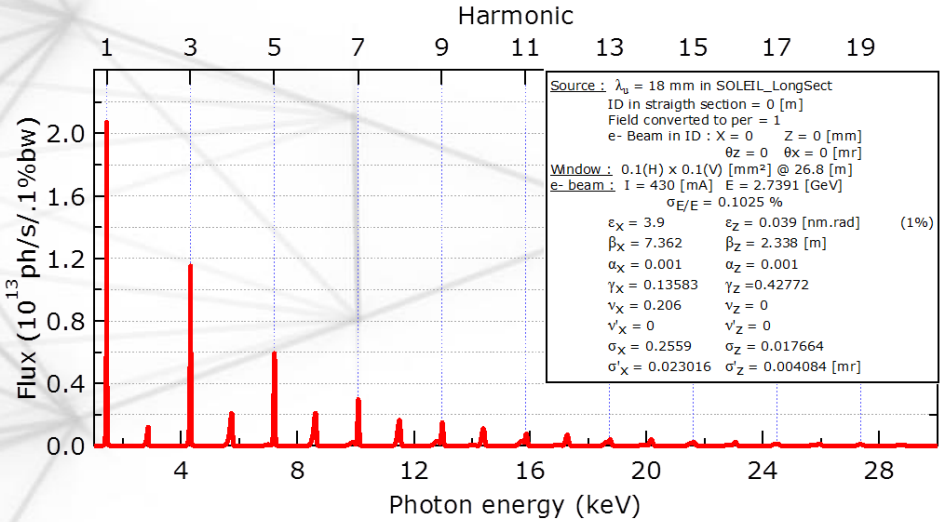

Figure 45 : *Radiation spectrum of the CPMU18#3 at 77 K*

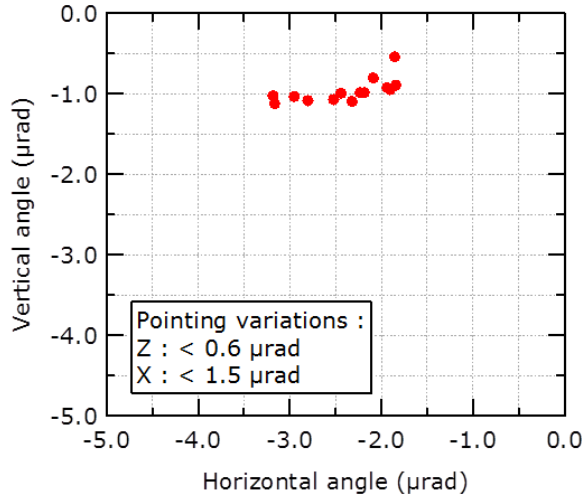

Figure 46 : *Pointing variations between 5.5 to 30 mm gaps*

Electrons beam based alignment

- Mech. Alignment for meas bench
- Electron beam alignment
  - Electron beam decay
  - Vertical betatron tune shift vrariations

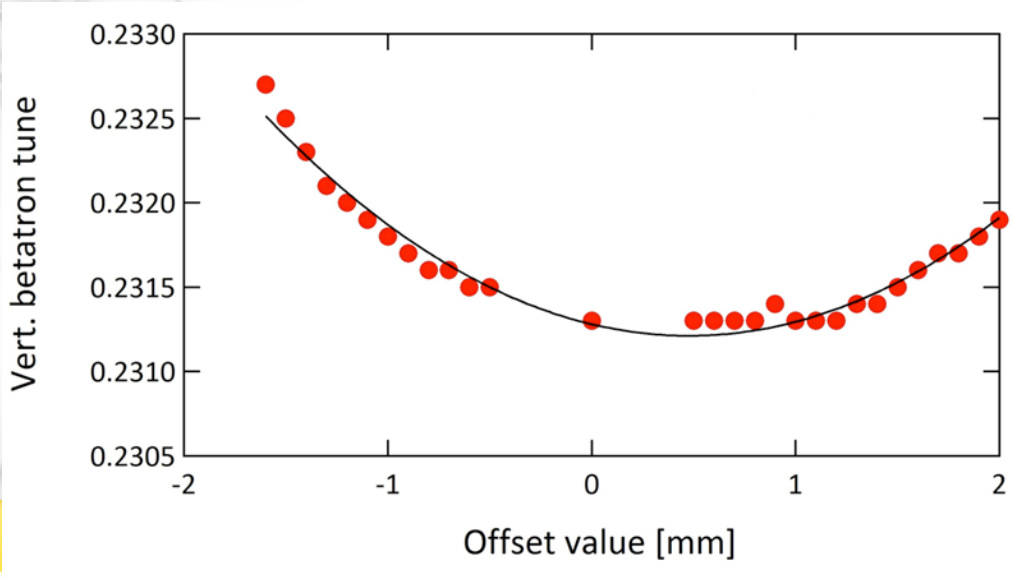

Figure 47 : *Betatron tune shift variations while moving the offset of the CPMU18#1*

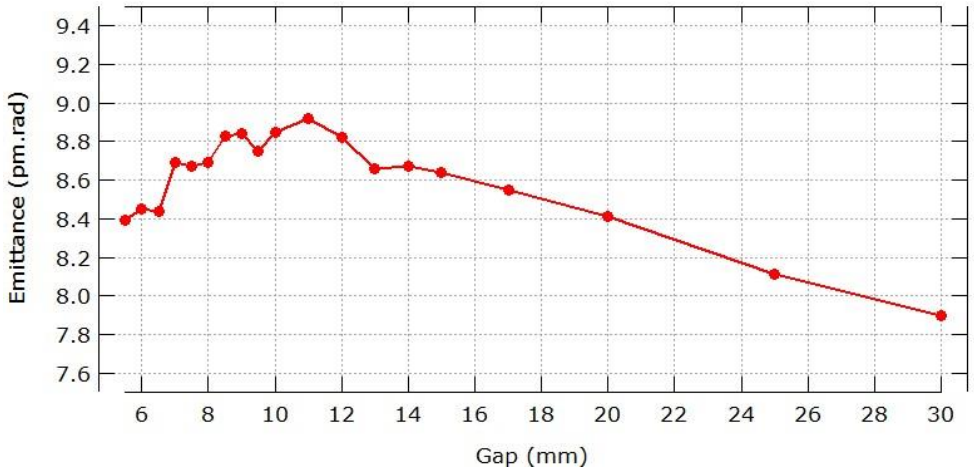

Figure 48 : *Vertical emittance variations versus gap of CPMU18#3*

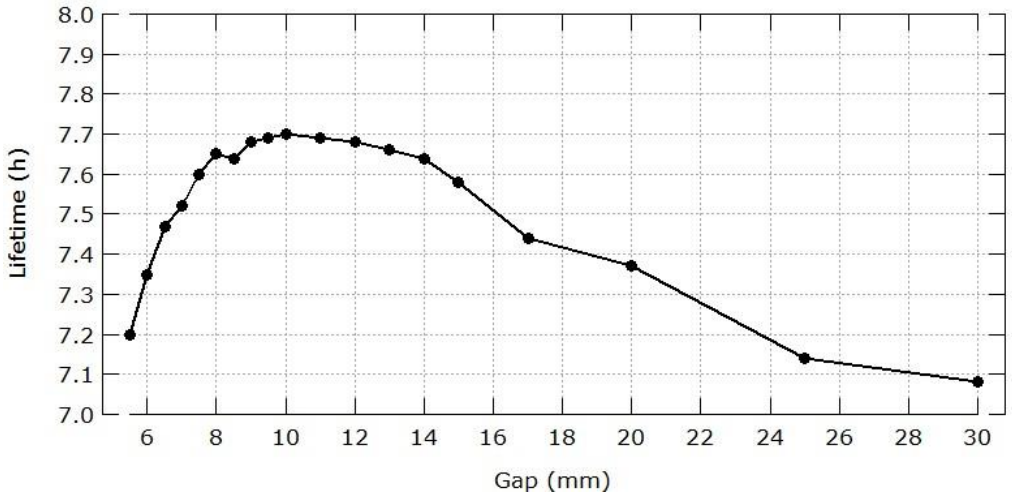

Figure 49 : *Lifetime variations versus gap of CPMU18#3*

Installation on the ring

Photons beam based alignment : offset adjustment

- Observation at 77 m from the source point
- Observation slit : 100 um x 100 um
- 11th harmonic at 16.5 keV

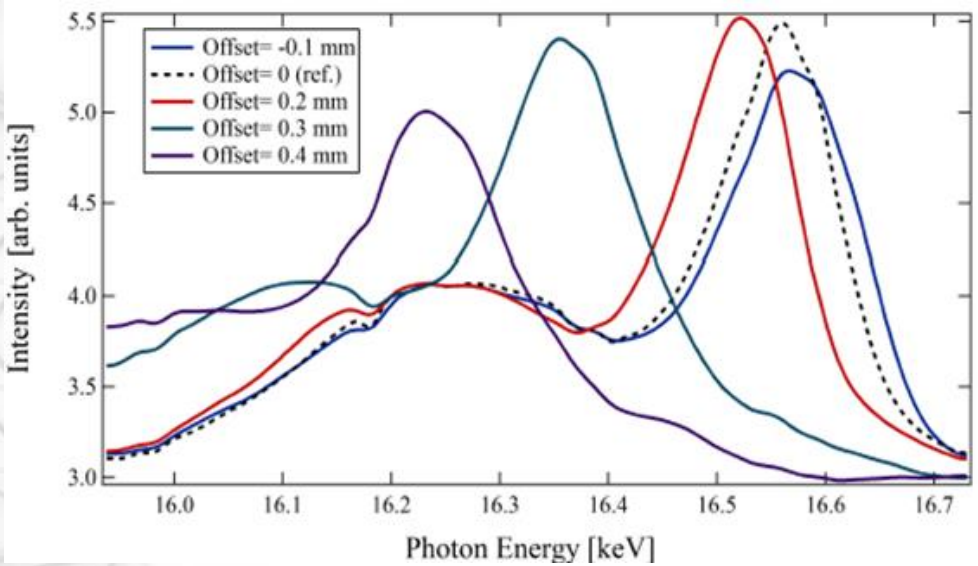

Figure 50 : *11th harmonic of the CPMU18#1 while moving offset from -0.1 to 0.4 mm*

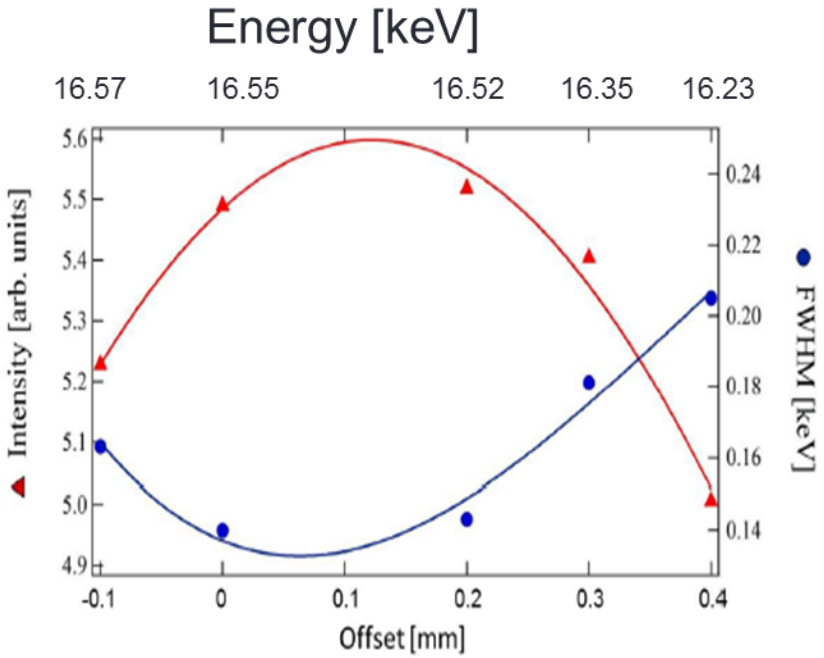

❖ New offset : 100 μm

Figure 51 : *Energy and bandwith of the 11th harmonic of the CPMU18#1 while moving the offset from -0.1 mm to 0.4 mm*

Photons beam based alignment : taper adjustment

- Change the peak field along the longitudinal axis
- Taper can be changed between +/-500 um

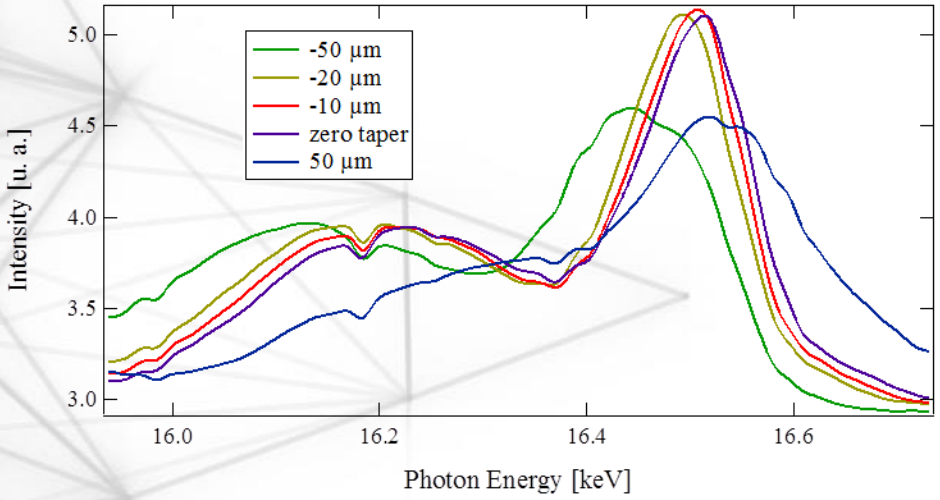

Figure 52 : *11th harmonic of the CPMU18#1 while changing the taper from -0.05 mm to 0.05 mm*

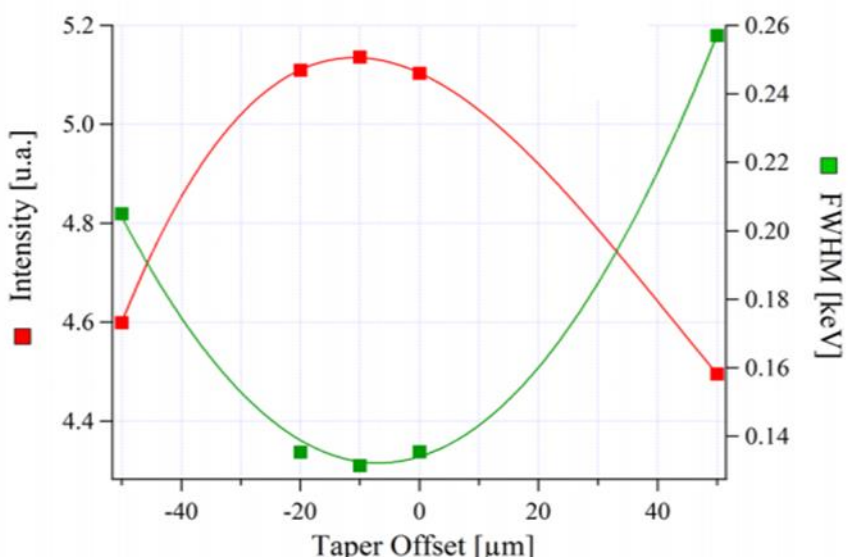

Figure 53 : *Energy and bandwith of the 11th harmonic of the CPMU18#1 while moving the taper from -0.05 mm to 0.05 mm*

Installation on the ring

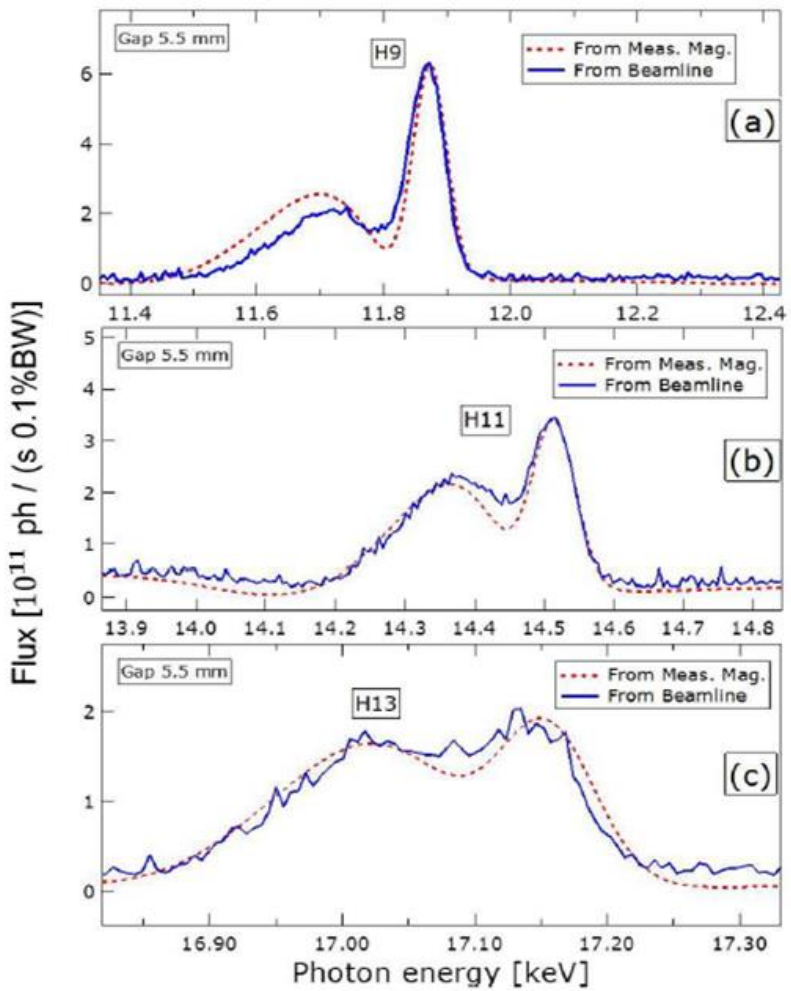

Figure 54 : *Comparison of the spectra of CPMU18#1 calculated from magnetic meas. using SRW and the one measured on Nanoscopium beamline at 5.5 mm gap*

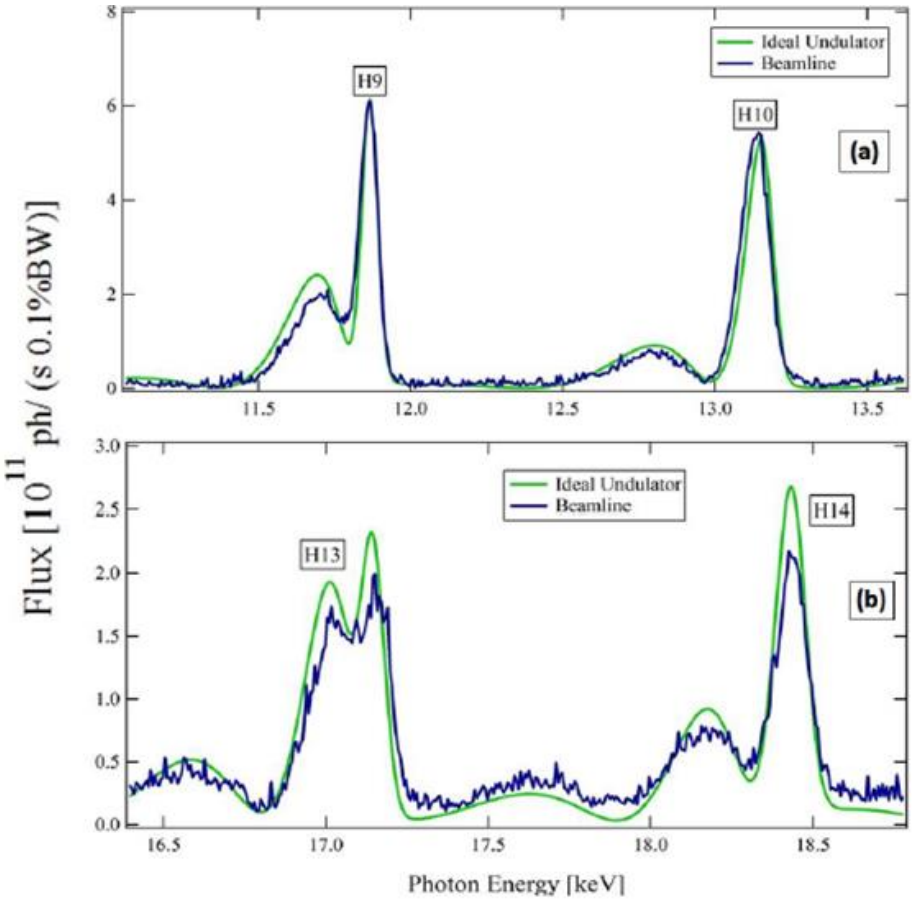

Figure 55 : *Comparison of spectra of an ideal CPMU18 and the one measured on Nanoscopium beamline at 5.5 mm gap*

Conclusion

CPMU18#1

- First full-scale PrFeB CPMU in operation since 2011 for Nanoscopium beamline
- Photon beam alignment with the beamline have been performed
- The quality of the CPMU is in good agreement with the calculations

CPMU18#2

- Low phase error value has been achieved directly after assembly
- Radiation has been observed on COXINEL experiment with a LPA beam after 8m of controlled electron beam transport
- Will be installed on the ring this summer 2024

CPMU18#3

- Low phase error value has been achieved directly after assembly
- Installed on the ring since 2018
- Electrons and photons beams measurements are in good agreement with what was expected

CPMU15#1

- Low phase error value has been achieved directly after assembly
- Has to be cooed down

CPMU12 (LEAPS)

- New design implemented with Supermodules (can be optimized and measured with a robot)
- 1m long prototype will be ready T4 2024
- New Hall probe bench is under design to be tested on this prototype